Journal of Intelligent Systems and Internet of Things
Vol. 17, No. 01, PP. 57-74, 2025
DOI: https://doi.org/10.54216/JISIoT.170105

# Park-Net: Multi-modality qEEG and fMRI-based PDDiagnosis via Attentional Graph Convolutional Neural Network

**S. Mohanapriya[1,*], Kamalraj Subramaniam[2]**

[1]Research scholar, Department of Computer Science and Engineering, Karpagem Academy of Higher Education, India

[2]Professor and Head, Department of Biomedical Engineering, Faculty of Engineering, Karpagam Academy of Higher Education, India

Emails: smohanapriya3@gmail.com; kamalrajee@gmail.com

**Abstract**

Parkinson's disease (PD) is a degenerative neurological condition instigated by the death of dopamine-producing neurons in the brain, which is manifested as tremors, rigidity, bradykinesia, and postural instability. Early and accurate diagnosis of PD is crucial for timely initiation of appropriate treatment strategies, which can help alleviate symptoms, advance excellence of life, and hypothetically leisurely disease development. A promising method for PD diagnosis is the combination of fMRI and qEEG methods, which provide full neuroimaging data to improve accuracy and early detection. However, recent studies are limited in performing and achieving accurate PD diagnosis. To alleviate this issue, we have proposed graph neural network-based PD diagnosis model addressed as Park-Net. Here, data pre-treatment is initially implemented in which both collected qEEG signal and fMRI image is denoised using Discrete Wavelet Transform (DWT) and Improved Kalman Filter (IKF) respectively. Following that, appropriate region of fMRI is segmented by adversarial network-based U-Net (AN-Net). After that, segmented region is fed into proposed Park-Net model; here modality encoder (ME) encompassed Long Short-Term Memory (LSTM) for feature extraction. We adapted Multi-modal Fused Attentional Graph Convolutional Neural Network (MAGCN) for constructing graph based on feature correlation and then fused. Finally, we designed Self-Attention Pooling with softmax layer for classifying PD as normal or abnormal. We have implemented our proposed Park-Net model to evaluate model performance, and its efficacy is assessed using a range of performance metrics such as accuracy, sensitivity, specificity, F1-Score, and ROC curve, highlighting its superior performance compared to existing methods in PD diagnosis approaches.

**Received: January 29, 2025 Revised: March 01, 2025 Accepted: April 07, 2025**

**Keywords:** Multi-modal; Parkinson’s disease; qEEG and fMRI; Attentional Graph Convolutional Neural Network; Self-Attention

## 1. Introduction

Parkinson's disease, a neurodegenerative disorder affecting movement, manifests with tremors, stiffness, and balance issues due to dopamine-producing neuron loss. Typically diagnosed in individuals over 60, it can also affect younger people. Though its exact cause remains unclear, genetic and environmental factors are implicated. Treatment aims to alleviate symptoms through medications, physical therapy, and sometimes surgery. Parkinson's presents significant challenges to daily life, affecting both physical and mental well-being. Ongoing research seeks to unveil new therapeutic approaches and deepen our understanding of this complex condition. Early and precise diagnosis is essential for timely intervention and enhanced patient outcomes. Prompt recognition of symptoms enables timely initiation of suitable treatments for effectively managing both motor and non-motor symptoms. Early diagnosis grants patients access to support services, personalized therapies, and lifestyle adjustments, thereby improving their quality of life. Additionally, it facilitates participation in clinical trials, driving advancements in Parkinson's research. Early intervention aids in mitigating potential complications, ensuring improved long-term management and potentially slowing disease progression. In summary, prompt identification of PD empowers individuals to proactively confront the challenges associated with this neurodegenerative condition.

The integration of qEEG (quantitative-electroencephalogram) and fMRI (functional-magnetic resonance imaging) provides a comprehensive diagnostic approach for Parkinson's disease. qEEG assesses brain electrical activity, detecting abnormal patterns suggestive of Parkinson's. Meanwhile, fMRI offers detailed structural images, assisting in the exclusion of other conditions and identifying specific brain changes linked to Parkinson's. By combining these methods, diagnostic accuracy is enhanced, facilitating early detection of the disease. This multi-modal approach not only aids in distinguishing PD from other disorders but also facilitates the development of personalized treatment plans. Diagnosis based on qEEG and fMRI contributes to a deeper understanding of Parkinson's, enhancing patient care through timely and precise interventions. Implementing a multi-modality approach, particularly employing a Graph Convolutional Neural Network (GCNN) with qEEG and fMRI data, improves accuracy by addressing previous research limitations. While qEEG traditionally struggles with spatial precision, integrating fMRI data provides detailed anatomical context, compensating for qEEG's spatial resolution limitations. Prior studies often focused on isolated features from qEEG or fMRI, whereas GCNN excels at capturing intricate relationships within complex datasets, enabling holistic feature extraction. Given Parkinson's dynamic temporal changes, this comprehensive approach enhances our ability to monitor disease progression effectively. The high temporal resolution of qEEG complements the static nature of fMRI, offering a more holistic view of the disease trajectory. Integrating information from qEEG and fMRI necessitates advanced techniques, where GCNN excels in cross-modal fusion, harnessing the advantages of both modalities for a synergistic diagnostic approach. Single-modal methods may struggle to differentiate PD from other neurodegenerative disorders, whereas the combined power of qEEG and fMRI within a GCNN framework enhances discriminatory capabilities, reducing the risk of misdiagnosis. Parkinson's impacts neural networks, and GCNN, tailored for graph-structured data, enables a nuanced analysis of network-level changes, shedding light on the disease's intricate connectivity patterns. Employing GCNN with qEEG and fMRI maximizes each modality's strengths, compensating for their limitations. This multi-modal approach yields a more accurate, comprehensive, and nuanced diagnostic strategy for Parkinson's, promising advancements in early detection and personalized treatment. The major research contributions are:

- ✓ To achieve enhanced PD diagnosis performance, we proposed several contributions including,
- ✓ Introduction of Park-Net: We introduce Park-Net, a novel graph neural network-based model for PD diagnosis, integrating data from qEEG signals and fMRI images.
- ✓ Data Pre-treatment: We employ Discrete Wavelet Transform (DWT) and Improved Kalman Filter (IKF) for denoising qEEG signals and fMRI images, respectively, ensuring high-quality data input for subsequent analysis.
- ✓ Advanced Model Architecture: Our model incorporates an adversarial network-based U-Net for fMRI region segmentation, a modality encoder (ME) with Long Short-Term Memory (LSTM) for feature extraction, and a Multi-modal Fused Attentional Graph Convolutional Neural Network (MAGCN) for constructing and fusing feature correlations in a graph-based representation, culminating in Self-Attention Pooling for accurate PD classification between normal and abnormal cases.

The structure of the remaining paper is organized as follows: Literature Review (Section II): This section extensively explores prior research on PD classification. Research Methodology (Section III): Here, we provide a detailed description of the methodology utilized within the Park-Net model, including mathematical equations, pseudocode, and diagrams for clarity. Experimental Results (Section IV): This section presents a concise summary of the experimental findings, including a discussion of performance metrics and a comparative analysis of outcomes. Discussion of Findings (Section V): Section V thoroughly discusses the findings from our proposed approach, offering insights and interpretations of the results. Concluding Remarks (Section VI): Finally, Section VI summarizes the key insights and implications drawn from the study, encapsulating our research is concluding remarks.

These Human beings have the information about heredity commonly saved in the gene. This kind of disease generates a disorder in the human body's expressions of the gene because of the mutation in one gene, a combination of gene mutation, different gene mutations, and different factors related to environments and damage to chromosomes. Few mutations or genetic disorders are the reason for developing human body cancer [1]. In addition, the gene mutation turns into a different new virus generation. This kind of change is mentioned in hereditary cancer syndromes, which are transferred to the child from the parents. Due to the genetic disorder, this kind of bone marrow cancer is called leukemia [2]. The leukemia risk is increased by the factors of the environment and the human being's lifestyle. The stem cell leads to the cancerous cell and slowly multiples it uncontrolled at the primary phase of leukemia. It has no factors, which are aware. Cancer cells are not working in a relevant way and use the healthy cells in the bloodstream and the bone marrow. Leukaemia is developed in the human body, is the fundamental factor is the cell mutations in the bone marrow. The healthy cells are developed using the bone marrow; this is thwarted. DNA mutation as deoxyribonucleic acid is detected, which is difficult for different genetic diseases for the earlier diagnosis due to the many genes that have multiple areas from where the mutation occurs [3]. One upgraded methodology is the DNA microarray that measures the expression level for the huge volume of genes. The ability to evaluate if individual DNA has the gene of mutation or not using technology. Various kinds of leukemia are used in microarray prediction and analysis technology [4].

The difficult task is the earlier prediction in today's world for physicians and adopting automatic computer oriented for disease diagnosis systems in the clinical phases. Various machine learning (ML) approaches are adopted to model the intelligent diagnosis system for clinical datasets. A large volume of data is created from the clinical sectors because of the upgrade and digital revolution in information technology. The large data is analysed, and different approaches are used to diagnose diseases called machine-

learning approaches [5] - [6]. Various data for the diagnosis are used in medical records forms at different hospitals for the successful run of machine learning algorithms. Microarray technology generates a large volume of DNA expression in hospitals. The data classification and the automated analysis are important for decision-making and earlier diagnosis of genetic disease [7]. One of the many famous regions is gene expression data in studies in the analysis related to biomedical data based on machine learning. The data is analysed for various algorithms of machine learning [8]. The proposed DPDPM approach is employed for leukemia prediction. There are two kinds of leukemia with the assistance of deep neural networks: AML as acute myelocytic and ALL as acute lymphocyte [9] - [10]. The suggested methods have a classification performance that is satisfactory when compared with previous works described in the conclusion section. The major research gap occurs due as the earlier prediction of leukemia is more challenging for experts and it can be achieved effectually by the automated disease diagnosis system. Thus, there is a need of huge gene expression dataset. Since, the provided AML dataset shows less number of labelled samples, there is a need of suitable features for the smaller dataset, which potentially learn better feature representation from data for AML prediction. However, layer-level stacking for feature extraction generally provides superior representation of learning models which motivates to design DPDPM to learn the higher level features. In addition, it is proven that the multi-modal data works well compared to single model data. Thus, it makes better prediction/classification outcomes.

The proposed system has the below organizations. Section 2 presents the related literature. Suggested work is offered in section 3. Section 4 presents the outcomes that are achieved via the suggested method. The conclusion work is presented in work 5.

## 2. Related Works

### A. EEG-based PD Diagnosis

Rea et. Al [21] investigated the relationship between quantitative EEG (qEEG) measures and cholinergic basal forebrain atrophy in PD and mild cognitive impairment (MCI). The study hires advanced neuroimaging techniques to search the neural correlates of cognitive decline in PD and MCI. By adding EEG analysis with structural MRI data, the authors provide valuable visions into the neurobiological foundations of cognitive impairment in these requirements. However, further longitudinal studies are necessary to authenticate the results and clarify the potential clinical implications. Chang et. Al [22] proposed an advanced approach for PD credit using EEG data and a sparse graph convolutional neural network (GCNN) with attention devices. By leveraging the characteristic spatiotemporal dynamics of EEG signals and joining attention devices, the model attains extraordinary accuracy in PD classification. The study proves the efficiency of DL techniques in investigating EEG data for disease diagnosis. However, the generalizability of the model across diverse inhabitants and its presentation in real-world settings essential to be further assessed. Shah et. Al [23] introduced a compact deep hybrid network based on dynamical systems for categorizing Parkinson's disease-related EEG signals. By integrating dynamical systems theory with DL architectures, the proposed model efficiently captures the nonlinear dynamics characteristic in EEG data. The study proves promising outcomes in PD classification, highlighting the possible of hybrid approaches in disease diagnosis. However, comprehensive authentication studies across different datasets and comparative analyses with prevailing methods would strengthen the strength of the proposed model. Oh et. Al [24] presented a deep learning (DL) approach for diagnosing PD from EEG signals. The authors leverage convolutional neural networks (CNNs) to extract relevant features from EEG data and employ a DL framework for disease classification. The study demonstrates encouraging results in PD diagnosis, highlighting the utility of DL techniques in analyzing EEG biomarkers. However, further investigations are needed to assess the model's performance in heterogeneous patient populations and its scalability in real-world clinical settings. Naghsh et. Al [25] focused on spatial analysis of EEG signals for detecting PD stages. The authors propose novel spatial features extracted from EEG data to characterize disease progression and classify different stages of PD. By incorporating spatial information into the analysis, the study offers insights into the spatial distribution of neural abnormalities associated with PD. However, the clinical utility of the proposed spatial features and their generalizability to diverse patient cohorts warrant further validation through longitudinal studies and clinical trials.

Shaban et. al [26] presented a novel approach to automating the screening process for PD through the utilization of DL techniques applied to electroencephalography (EEG) data. The authors propose a DL model capable of accurately distinguishing between PD patients and healthy individuals based on EEG signals. The study demonstrates promising results, suggesting that EEG-based automated screening holds potential for improving the efficiency and accuracy of PD diagnosis. The integration of DL methodologies with EEG data highlights a significant advancement in the field of neurodegenerative disease diagnosis. Khare et. al [27] introduced an advanced approach for noticing PD by engaging an automated tunable Q wavelet transform technique with EEG signals. The study discovers the efficiency of this method in differentiating PD patients from healthy controls based on EEG data analysis. By leveraging advanced signal processing techniques, the authors prove promising results in exactly identifying PD patients. The proposed method offers a non-invasive and effective means of diagnosing PD, possibly leading to earlier detection and interference, which are vital for improving patient results. Massa et. al [28] investigated the utility of quantitative EEG (qEEG) in the early discovery of Lewy body disease (LBD), a common neurodegenerative disorder thoroughly related to Parkinson's disease. The study discovers the potential of qEEG procedures as biomarkers for classifying early-stage LBD. Through comprehensive analysis, the authors deliver indication supporting the use of qEEG in detecting subtle neurological variations associated with LBD, thereby facilitating early diagnosis and involvement. The findings underscore the importance of qEEG as a valued tool in the clinical

valuation of neurodegenerative diseases beyond Parkinson's. Rea et. al [29] investigated the relationship between quantitative EEG procedures and cholinergic basal forebrain atrophy in persons with PD(PD) and mild cognitive impairment (MCI). The study discovers the potential of qEEG as a biomarker for evaluating cholinergic system dysfunction, which is implicated in cognitive decline in PD and MCI. Through advanced neuroimaging techniques and EEG analysis, the authors demonstrate associations between qEEG abnormalities and cholinergic basal forebrain atrophy in PD and MCI patients. These results highlight the utility of qEEG in clarifying the neurobiological devices underlying cognitive impairment in PD and MCI inhabitants, with implications for early diagnosis and targeted involvement. Overall, these research papers collectively contribute to advancing our understanding of PD diagnosis and management through innovative EEG-based approaches. By harnessing the power of deep learning, signal processing techniques, and neuroimaging methodologies, these studies offer promising avenues for improving the accuracy, efficiency, and early detection of PD and related neurodegenerative disorders [30].

### C. EEG-MRI-based PD Diagnosis

Early and accurate diagnosis of PD, especially in its prodromal stages or when accompanied by cognitive decline, remains a significant challenge in clinical practice. Two recent research papers have explored innovative approaches utilizing neuroimaging techniques, namely EEG and fMRI, alone and in combination with MR imaging, for the diagnosis of PD and its association with mild cognitive impairment (MCI). The author focused on the utilization of EEG and fMRI as standalone modalities for the diagnosis of PD. EEG procedures the brain electrical activity, while fMRI captures changes in blood flow, providing insights into neural activity. The paper presents promising results in identifying specific patterns of neural activity associated with PD, suggesting the potential of these techniques as non-invasive diagnostic tools. However, challenges such as standardization of protocols and variability in patient populations need to be addressed for broader clinical applicability. He investigated the synergistic use of MR imaging and EEG for noticing PD with MCI. By mixing structural and functional brain imaging data with EEG biomarkers, the study aims to improve diagnostic precision, particularly in differentiating PD patients with cognitive impairment. The combined approach proves enhanced sensitivity and specificity associated with individual modalities, contributing to a promising avenue for early detection and intervention in PD patients with cognitive decline. Both research papers underscore the potential of advanced neuroimaging techniques in revolutionizing the diagnosis and management of PD. By elucidating distinct neural signatures associated with the disease, these studies pave the way for personalized medicine approaches and targeted interventions. However, further validation through large-scale clinical trials and longitudinal studies is necessary to establish the robustness and reliability of these techniques in diverse patient populations. Additionally, efforts towards standardization of protocols and integration with other clinical measures are essential for translating these findings into routine clinical practice. Overall, these research endeavors represent significant strides toward advancing our understanding and treatment of PD and its associated cognitive impairments.

## 3. Methodology

In this research, multimodality data of fMRI and qEEG signal based PD diagnosis model is designed. Here, we performed several process including as data pre-treatment, segmentation and reconstruction followed by Park-Net based PD classification that are detailed in following sub-sections. Fig 1 illustrates the overall workflow of proposed Park-Net model.

### 3.1 Data Pre-Treatment

qEEG Denoising: We employ the Discrete Wavelet Transform (DWT) technique to filter noise from the acquired qEEG signal. This approach excels in preserving signal characteristics across both frequency and temporal domains. The original Signal is denoted, as Sign (x) can be disintegrate for denoising

$$\mathrm{Sign(x)} = \sum_{y=-\infty}^{\infty} \mathrm{sa_y} \not\subset (\mathrm{x} - \mathrm{y}) + \sum_{i=-\infty}^{\infty} \mathrm{er_{i,y}} \not\supset (2^{\mathrm{i}}\mathrm{x} - \mathrm{y}) \quad (1)$$

From this equation, $\mathrm{sa_y}$ and $\mathrm{er_{i,y}}$ represents the coefficient of scaling and wavelet respectively. $\not\subset$ and $\not\supset$ denotes the function of scaling and wavelet respectively. Sign(x) is the first part in the above equation provides the utmost details of the incoming signal. Whereas, the second part of the equation $\mathrm{er_{i,y}} \not\supset (2^{\mathrm{i}}\mathrm{x} - \mathrm{y})$explains the error among the signal and noise respectively in terms of i and $\mathrm{i} - 1$ scales respectively. To refine, the Daubechies wavelet, specifically with scale numbers I to 5, serves as the foundational wavelet $\not\supset$ for denoising signals. Here, 'WC' and 'WAC' denote wavelet and wavelet approximation coefficients, encompassing coefficients (WC1-WC5 and WAC5) representing different scales. By nullifying computed coefficients, noise within the input signal is effectively eradicated. Consequently, this process allows for the elimination of redundant and fluctuating information inherent in the initial qEEG signals, thereby enhancing denoising.

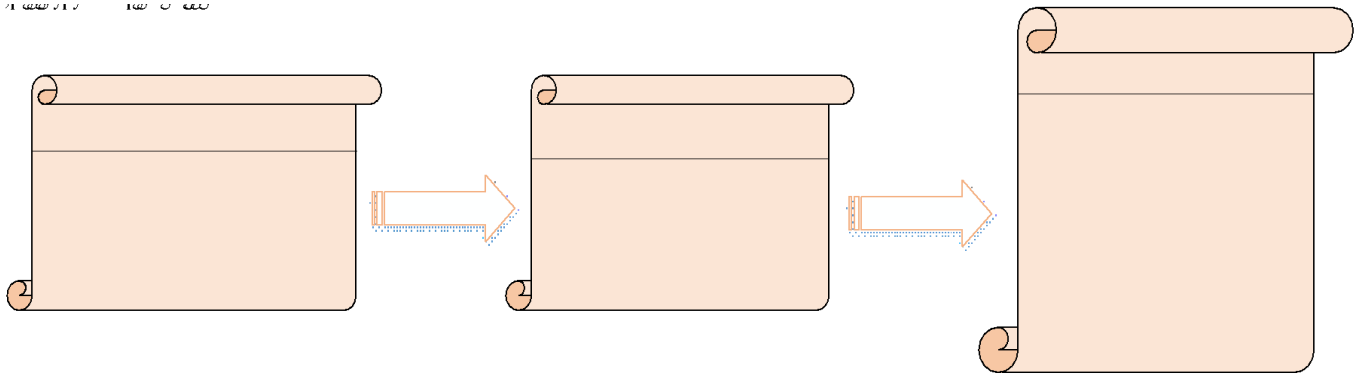

**Figure 1.** Overall Workflow of Park-Net based PD Diagnosis

fMRI Denoising: In fMRI scans, various types of noise can be detected, such as salt and pepper, Ricin noise, Gaussian noise, and sparkle noise. Enhancing the quality of MRI images necessitates the removal of these noise artifacts. We propose employing Improved Kalman Filters (IKF) for this purpose. IKF effectively smoothens the image and suppresses noise while preserving edge features. Specifically, IKF operates by removing noise from the linear system, optimizing image utilization, and complementing its function with a Gaussian filter. This combined approach enhances the efficacy of the system's current state assessment and the overall image quality. The images is completed to spatially be contingent on present pixel $\psi(x-t)(y-h)$ for $(t,h) \in \aleph$ and this is mathematically represented as,

$$\psi(x-y) = \sum_{(t,h)\epsilon\aleph}^{n} \mu_{t,h}\psi(x-t)(y-h) + o(x-y) \quad (2)$$

From the aforementioned equation, $\aleph$ indicates the pixels range neighbouring $\psi(x-y)$ utilized in sum of linear and $(t,h)$ is the coordinate centred at present pixel $\psi(x-y)$. $o(x-y)$ denotes resultant noise and it is contemplated as white noise consuming zero mean while greater $\aleph$ is chosen. Image reconstruction enhances noise removal by eliminating artifacts such as blurriness and additive noise from the noise-reduced image.

$$\psi(\nexists) = \omega Y(\nexists - 1) + \lambda(\nexists) \quad (3)$$

Where,

$$\psi(\nexists) = [Y_0(\nexists), Y_1(\nexists), \dots, Y_8(\nexists)]^H \quad (4)$$

The above-mentioned equation is illustrated as state variable on time $\nexists$ . By this way, the noise presented in MRI images are removed.

### 3.2 Segmentation & Reconstruction

fMRI Segmentation: We have devised a novel framework for tumor segmentation in MR images by integrating two established techniques: Adversarial networks (AN) and the U-net approach. Our approach combines the encoder-decoder structure of U-net with tensors from AN, utilizing skip connections for improved segmentation accuracy. The AN-net architecture comprises an encoding part (synthetic upsampling) and a decoder component (analytic downsampling), as illustrated in Figure 2. Within each of the five encoder blocks, we employ double convolutions enhanced by batch normalization and rectified linear unit (ReLU) activation function, followed by max-pooling, as described in equation 6. The output from each encoder block is concatenated with its respective input, n ith the input being interpolated to align with the feature map of the output.

$$\mathrm{ReLu}(x) = \{0, \quad x \le 0\ x, \quad \text{otherwise} \quad (5)$$

$$\sum_{n=1}^{x}(x) = \frac{1}{1+e^{-x}} \quad (6)$$

$$l_n = -z_n[h_n.\log\log x_n + (1-h_n).\log(1-x_n)\,] \quad (7)$$

Here, z denotes optimal weight, h and x are target and input. Furthermore, the decoder part comprise of five blocks, the similar as encoder block, excluding for utilize of Conv-Transpose2d replacing max pooling. To recover the original dimensions of the image within the final decoder block, we typically employ Conv-Transpose2d to upscale the tensor at the conclusion of each decoder

block. The output block, situated at the end of this sequence, consists of a sigmoid activation function combined with a single convolution. For training, we employed the adaptive moment estimation (ADAM) optimizer, utilizing a batch size of 32 and the binary cross-entropy loss function on 3 channels of 128 × 128 pixels. The model underwent training for 200 epochs.

### 3.3 Park-Net based PD Diagnosis

Following that, we fed our enhanced data into proposed Park-Net, which encompasses of Multi-modality Encoder (ME) for capturing imperative features from both inputs followed by Multi-modality Attentional-Graph Convolutional Neural Network (MAGCN) for generating the graph based on features correlation to fusion. At last, Multi-modality Decoder (MD) with softmax layer analysis the fused feature map and then classifies PD, which are detailed as follows. Figure 3 represents the architecture of proposed Park-Net.

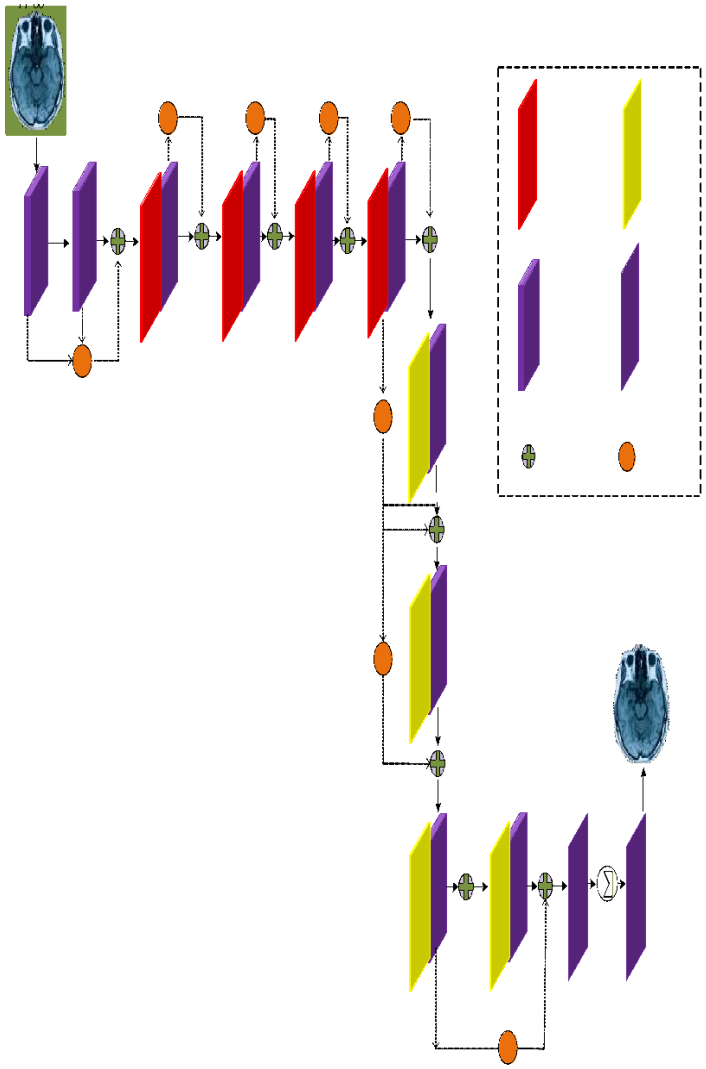

**Figure 2.** Encoding and Decoding component

#### (i) Modality Encoder

As mentioned earlier, incorporating spatial-temporal information is crucial for predicting the PD. Thus, it's advantageous to integrate spatial-temporal information into the feature representation of abnormality. We achieve this by generating spatial-temporal-aware feature encoding for each modality using corresponding modality encoders. Specifically, we utilize a bidirectional Long Short-Term Memory (LSTM) network to encode spectral-temporal information for the both qEEG and fMRI modalities. The formulation of spatial-temporal-aware feature encoding for individual data can be expressed as follows:

$$h_i^{qEEG} = \left[\overrightarrow{LSTM}\left(u_i^{qEEG}, h_{i-1}^{qEEG}\right), LSTM^{\leftarrow}\left(u_i^{qEEG}, h_{i+1}^{qEEG}\right)\right] \quad (8)$$

$$h_i^{fMRI} = W_e^{fMRI} u_i^{fMRI} + b_i^{fMRI} \quad (9)$$

Here, $u_i^{qEEG}$ and $u_i^{fMRI}$ are the spectral-temporal raw feature depiction of data i from qEEG and fMRI modalities, respectively. The encoder of modality outputs the spatial-temporal-aware encoding of feature $h_i^{qEEG}$ and $h_i^{fMRI}$ correspondingly.

**(ii) Multi-modal Fused AGCN**

To capture spatial-temporal dependencies across multiple modalities at the data level, we introduce a Multimodal fused Attentional Graph Convolutional Network (MAGCN). Furthermore, we employ a spectral domain graph convolutional network to encode multimodal spatial-temporal information. Additionally, we deepen the network by stacking more layers to create a deep Attentional-GCN which we have detailed in following sub-division;

Graph Construction: A data with N information can be described as undirected graph $G = (V, Z)$, where $V(|V| = 3N)$ represents information nodes in both modalities and $\Phi \subset V \times P$ is a graph of relationships comprehending qEEG and fMRI modality dependency. We generate graph as follows,

Nodes & Edges: Each information (feature) is denoted by two nodes $y_i^{qEEG}, y_i^{fMRI}$ in graph, initialized $h_i'^{qEEG}, h_i'^{fMRI}$ which refers $\left[h_i^{qEEG}, \S_i\right], \left[h_i^{fMRI}, \S_i\right]$ respectively, equivalent to two modalities. Henceforth, providing a data with N information, we fabricate graph along with 2N nodes. Suppose that individual information has absolute connection to other information in same data. Thus, any two nodes of similar modality in same data are correlated in graph. Besides, individual node is correlated with nodes which equivalent to similar information anyhow from diverse modalities.

Edge Weighting: We propose that a higher edge weight should be assigned to two nodes since their information exchange is more significant when they are more similar to each other. We use the edge weight between two nodes to calculate angular similarity, to measure the similarity of node representations. There are two different kinds of edges in the graph: (i) Nodes within the same modality are connected by edges, and (ii) Edges that join nodes with various modalities. In order to differentiate between them, we use different edge weighting schemes. The edge weight for the first kind of edges is computed as follows:

$$\Psi_{ij} = 1 - \frac{\arccos\left(\mathrm{sim}(n_i, n_j)\right)}{\vartheta} \quad (10)$$

From the abovementioned equation, $n_i$ and $n_j$ indicates feature depictions of i-th and j-th graph. For the second kind of edges, the edge weight is generated as,

$$\Psi_{ij} = ¥\left(1 - \frac{\arccos\left(\mathrm{sim}(n_i, n_j)\right)}{\vartheta}\right) \quad (11)$$

Where ¥ is the hyperparameter.

MAGCN: Equation 12, which uses a k-hop information aggregation technique to allow node representations to collect local structural information up to k-hop neighbors, is the foundation of the most common approach in graph neural networks. But as the number of layers increases, a considerable amount of original information is lost at each convolution step, which reduces the model's capacity and affects prediction accuracy. Our attention graph convolution (AGC) layer presents a basic idea intended to improve model performance in order to overcome this constraint. AGC seeks to extract meaningful information from each individual hop, as opposed to merely depending on the k-hop convolution result. This results in a hierarchical representation that includes the most important information from many convolution operations across distinct hops. We show attention approach and accomplish it on equ (12) to generate node indication $\gamma_{\alpha_n}$ as,

$$\gamma_{\alpha_n} = \sum_{i=1}^{k} \beta_i H_{\alpha_n}^k \quad (12)$$

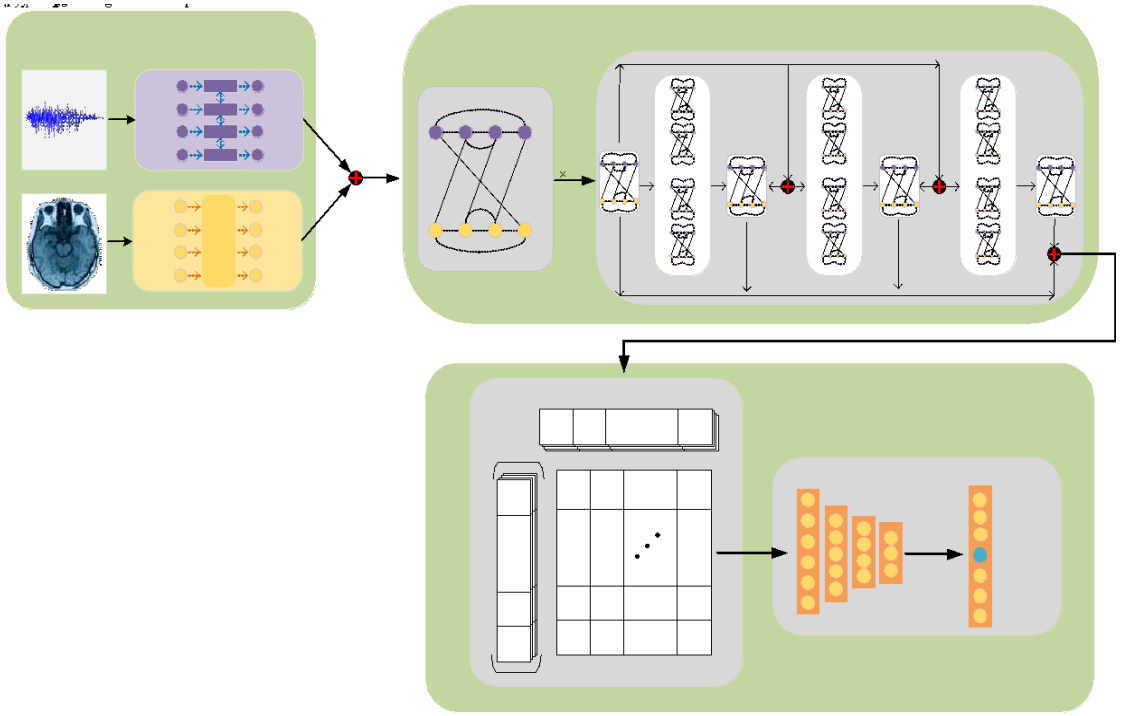

**Figure 3.** Architecture of Proposed Park-Net Model

For the sake of simplicity, we employ vanilla attention to ascertain the significance of each hop's aggregation result, where α represents the attention weight and $H_{\alpha_n}^k$ denotes node $\alpha_n$'s local structure within k hops. The resulting node representation encompasses the hierarchical structural information. Figure 2 provides a comparison between the traditional convolution layer and the attention convolution layer. We use the Residual Learning technique by stacking ϖ attention convolution layers to fully utilize the advantages of DL and uncover deeper latent features. The end result of this process is the creation of an attention graph convolutional module that is intended to improve the final node representation, represented by the symbol $\alpha_n$. The total of the output from the previous layer and the initial input X is what each AGC layer receives as input. As can be seen in the Attention Graph Convolution Module shown in Figure 1, we then use a dense layer to process the combination of outputs from each convolutional layer.

$$\gamma_{\alpha_n}^{\varpi+1} = \sum_{i=1}^{k} \beta_i H_{\alpha_n}^k \qquad H_{\alpha_n}^0 = \gamma_{\alpha_n}^{\varpi} + X \tag{13}$$

$$\gamma_{\alpha_n} = \mathrm{Dense}\left(\left\{\gamma_{\alpha_n}^0, \gamma_{\alpha_n}^1, \gamma_{\alpha_n}^2, \dots, \gamma_{\alpha_n}^m\right\}, \theta\right) \tag{14}$$

The outputs from every attention graph convolution layer are combined by a dense layer represented by the function Dense(). As a result, we achieve the node representation γ for every vertex $\alpha \in G$. To keep things simple, we depict the graph as a matrix G with size n-by-c dimensions, where each row represents a node.

$$G = \left(\gamma_{\alpha_1}, \gamma_{\alpha_2}, \dots, \gamma_{\alpha_n}\right) \tag{15}$$

**(iii) Self-Attention Pooling based PD Classification**

To effectively tackle the graph classification task, our aim is to derive a comprehensive graph-level representation from individual node representations. Traditionally, techniques such as sort pooling and mean/max pooling have been utilized to combine node representation vectors into a network representation vector. However, we propose a more efficient alternative to traditional pooling methods. Instead of employing max/mean pooling or pooling after sorting, which we deem unnecessary and inefficient, we advocate for the use of a self-attention pooling layer. Our objective is to enhance information retention in node representations during the encoding of a given graph into a fixed-size embedding matrix. Figure 3 illustrates the implementation of this method, displaying the creation of a coefficient matrix for the attention-pooling layer. In our approach, we leverage the attention mechanism, utilizing the graph node representations acquired from the convolution module as input to produce the weights vector ξ.

$$\varrho = \mathrm{softmax}\left(\lambda_2 \tanh(\lambda_1 G^T)\right) \quad (16)$$

Here, $\lambda_1$ and $\lambda_2$ are denoted as weight matrices with c-by-c and c-by-r respectively, in this r refers to hyperparameter which range for the number of subspaces for determining graph representation from node depiction. $\xi$ develops weight matrix replacing of vector and aforementioned equation can be mathematically rewritten as,

$$B = \mathrm{softmax}\left(\lambda_2 \tanh(\lambda_1 G^T)\right) \quad (17)$$

Individual row of B refers weight of single node's in diverse sub-space. The softmax function is implemented with second dimension of its input. Following that, a weighted summation corresponding to B from above-mentioned equation to acquire matrix of graph representation M with shape n-by-r.

$$M = BG \quad (18)$$

We have matrix of graph representation of that individual row is graph representation in single sub-space and the entire matrix generates inclusive for graph. Finally, fully-connected layer continued through softamx layer which takes M as input to implement graph classification (i.e., PD classification),

$$y' = \mathrm{softmax}(ZM + C) \quad (19)$$

Henceforth, we acquire result of final classification $y'$ which classifies normal or abnormal.

## 4. Result and Analysis

This section explains the experimental analysis of the proposed PD diagnosis model named Park-Net based on various scenarios and existing works. This section also sub-divided into three sub-sections, which includes implementation analysis, dataset details & performance metrics, and result analysis. The detailed discussion of those sections is provided below.

### A. Implementation Details

The implementation of the proposed Park-Net is carried out using python programming language with PyTORCH DL library. The hardware configuration includes Central Processing Unit (CPU) processor of AMD Ryzen 5 5600H with Radeon Graphics 3.30 GHz, The Random Access Memory (RAM) capacity of 8GB with NVIDIA GEFORCE GTX 32GB Graphics Processing Unit (GPU). The learning rate provided to the designed Park-Net is le-4 in which the Adam Optimizer is utilized with weight diminishing value of le-7. More clearly, this research tunes the software configuration in uniform manner with batch size of 5 to 50 respectively.

### B. Dataset Details & Performance Metrics

In this research, totally 80 PD(PD) were registered. Among that, 39 patients were resided in the Parkinson's Disease-Normal Cognition (PD-NC) whereas 41 patients were resided in the Parkinson's Disease-Mild Cognitive Impairment (PD-MCI). Table 1 represents the clinical and demographic of the patient data.

**Table 1:** Demographic and Clinical Data

| **Instance** | **PD-NC (n=39)** | **PD-MCI (n=41)** | *p value* |
|---|---|---|---|
| Maximum Mean Square Error | $30 \pm 2.3$ | $31.4 \pm 3.5$ | $< 0.002$ |
| Montreal Cognitive Assessment | $37.8 \pm 3.5$ | $34.8 \pm 5.5$ | $< 0.002$ |
| Light Emitting Diode mg/day | $434.68 \pm 426.44$ | $429.86 \pm 425.91$ | 0.050 |
| Unified Parkinson Rating Scale III | $30.07 \pm 9.8$ | $30.09 \pm 9.5$ | 0.036 |
| Duration of Years | $3.9 \pm 3.4$ | $4.7 \pm 4.7$ | 0.379 |
| Age in years | $68.1 \pm 12.0$ | $72.2 \pm 9.3$ | 0.106 |
| Gender (M/F) | 34/23 | 29/29 | 0.29 |

With those dataset details, we have evaluated the performance of the proposed model by adopting several validation metrics. The validation metrics includes ROC curve, F1-score, sensitivity, specificity, and accuracy respectively. The formulation of the performance metrics are provide as follow,

ROC Curve: Receiver Operating Curve (ROC) defines the ability of the PD classifier to the diagnose the disease based on the threshold. More clearly, higher the ROC performance higher the classification performance.

F1-Score: The F1-score is defined as the harmonic mean among the recall and precision rates. The F1-score is ultimately utilized for uneven distribution of classes. Higher the precision value better will be the performance. The formulation is provided as follows,

$$\mathrm{F1-score} = \frac{2 \times \mathrm{pre} \times \mathrm{rec}}{\mathrm{pre} + \mathrm{rec}} \qquad (20)$$

Recall: Recall defines the ability of the model to precisely identify the positive classes. The recall is computed by ratio of true positive samples to the amount of true positive and false negative rates respectively. The formulation of recall is provided as below,

$$\mathrm{rec} = \frac{\mathrm{T^{rp}}}{\mathrm{T^{rp}} + \mathrm{F^{ng}}} \qquad (21)$$

Precision: Precision rate defines the ability of the model to precisely identify the negative samples from the negative instances. The recall is computed by the ratio of the amount of true negative samples to amount of true negative and false positive samples respectively. The formulation of precision is provided as follows,

$$\mathrm{pre} = \frac{\mathrm{T^{ng}}}{\mathrm{T^{ng}} + \mathrm{F^{ap}}} \qquad (22)$$

Accuracy: The accuracy metric defines the amount of correct detection results to the overall detection results. The accuracy is computed by the sum of true positive and true negative rates to the ratio of sum of true positive, true negative, false positive, and false negative rates respectively. The formulation is provided as follows,

$$\mathrm{Acc} = \frac{\mathrm{T^{rp}} + \mathrm{T^{ng}}}{\mathrm{T^{rp}} + \mathrm{T^{ng}} + \mathrm{F^{ap}} + \mathrm{F^{ng}}} \qquad (23)$$

### C. Proposed Park-Net Model Evaluation

The designing of PD diagnosis model based on multi-modality framework named Park-Net emancipates clutches in the automated medical diagnosis paradigm. For disease diagnosis, we have acquired both signal and imagining modalities respectively named quantitative-electroencephalogram (qEEG), and functional Magnetic Resonance Imaging (fMRI). Since we acquired real time qEEG and fMRI data for the patients, the noise and irrelevant data holds a major issue. For that we have pre-process the multi-modality data by performing separate pre-processing techniques, for fMRI we perform noise removal, decomposition of cerebral cortex, and reconstruction whereas for qEEG we perform wavelet decomposition and reconstruction. The pre-processed data are then provided to the designed Park-Net module in which the proposed model possess encoder-decoder architecture with attention-based graph neural networks. The multi-modality is responsible for extracting the spectral and temporal features from both the modalities. Followed by the multi-modality attention-based graph neural network correlates the features from the both the inputs and fuse them to form the fused feature map. The fused feature map is then provided to the multi-modality decoder for effective Parkinson disease classification. The Park-Net consist of multi-modality attention GCN module for correlating the features of qEEG and fMRI based on its similarities. To be more specific, the GCN algorithm effectively correlates the relationship among the qEEG and fMRI features of the patients to form the fused feature map. The high precise fused feature map then fed to the decoder module for Parkinson disease diagnosis. For better understanding of the proposed Park-Net model, we have shown the effectiveness of proposed Park-Net in two scenarios named (a) Park-Net with Multi-Modality Attention GCN, and (b) Park-Net with GCN in table and figures respectively.

**Table 2:** Model Performance Evaluation

| Proposed Scenarios | Stages | Accuracy | Precision | Recall | F1-Score |
|---|---|---|---|---|---|
| Park-Net with Multi-Modality Attention GCN | Normal | 99.70% | 99.23% | 99.80% | 99.97% |
| | MCI | 99.17% | 99.27% | 99.37% | 99.03% |
| Park-Net without GCN | Normal | 96.47% | 95.26% | 95.43% | 95.08% |
| | MCI | 95.26% | 95.15% | 94.82% | 94.06% |

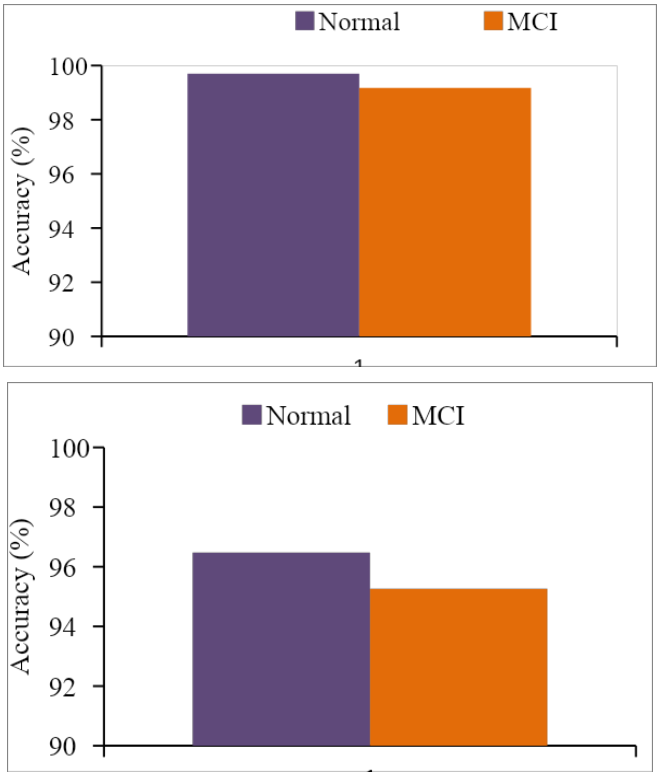


**Figure 4.** Performance Analysis of Accuracy (a) Accuracy with GCN & (b) Accuracy without GCN

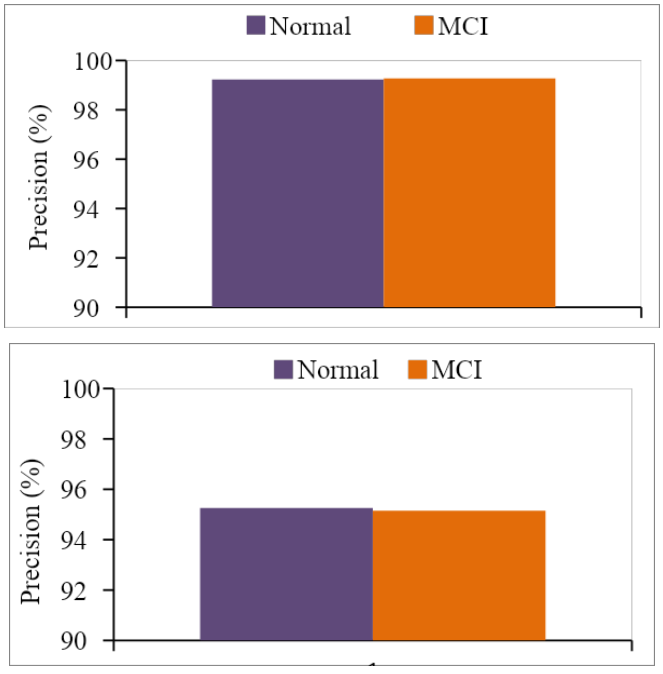


**Figure 5.** Performance Analysis of Precision (a) Precision with GCN & (b) Precision without GCN

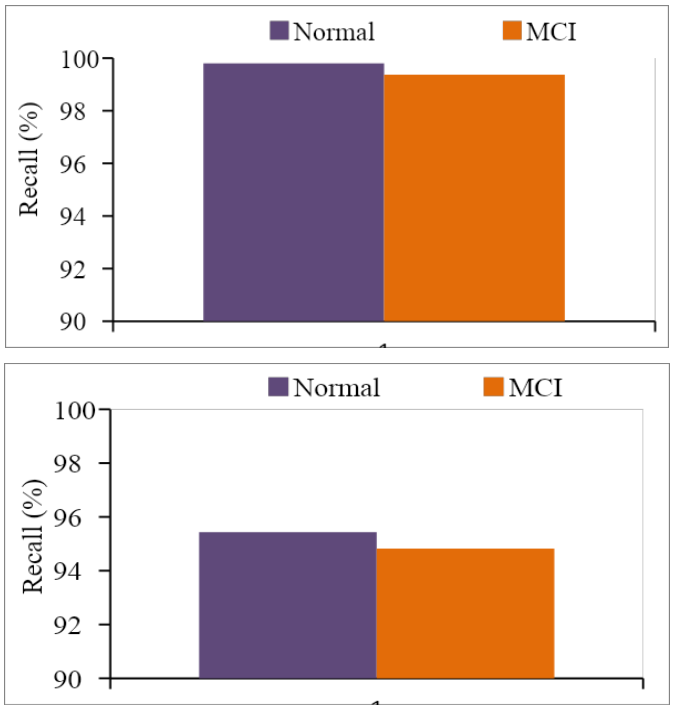


**Figure 6.** Performance Analysis of Recall (a) Recall with GCN & (b) Recall without GCN

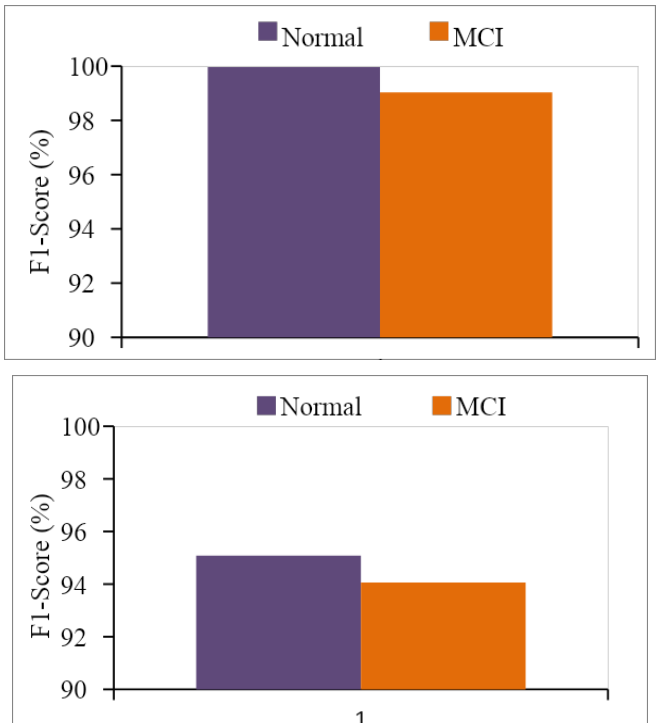


**Figure 7.** Performance Analysis of Recall (a) Recall with GCN & (b) Recall without GCN

Fig (4) - (7) shows the representation of effectiveness of the proposed scenarios in terms of four major metrics such as accuracy, precision, recall, and F1-score. The fig 4 (a) & (b) shows the accuracy of with multi-modality attention GCN and without GCN in which the scenario (a) shows better accuracy of 99.70% for the normal stage whereas without GCN scenario (b) achieves 96.47% for the normal stage. Furthermore, the MCI achieved by the scenario (a) and (b) are 99.17% and 95.26% respectively. The fig 5 (a) & (b) shows the precision comparison in which for the normal stage, the scenario (a) and (b) achieves 99.23% and 95.26%

respectively whereas for the MCI stage the scenario (a) and (b) achieves 99.27% and 95.15% respectively. The fig 6 (a) & (b) shows the recall comparison in which for the normal stage, the scenario (a) and (b) achieves 99.80% and 95.43% respectively whereas for the MCI stage the scenario (a) and (b) gains 99.37% and 94.82% respectively. Finally, the fig 7 (a) and (b) represents the F1-score comparison for scenario (a) and (b) in which normal stage gains 99.97% and 95.08% whereas for the MCI stage the proposed scenarios achieve 99.03% and 94.06% respectively. From the graphical and quantitative illustration, the scenario (a) gains better performance than the scenario (b) due to adoption of multi-modality attention GCN that firmly captures the important features correlations from qEEG and fMRI inputs.

### D. Comparative Analysis

In this sub-section, we examine the performance of the proposed Park-Net with the existing works such as CNN-PD [24], Spatial-PD [25], DL-PD [33], LSTM-PD [37], Standalone-PD [39], and Combine-PD [40]. The illustration of the performance metrics in terms of figures and table are provided as follows. From the figure (8) - (12) and table (3) – (6), we assess the performance of the proposed and existing works using various performance metrics. From the illustrations and quantitative analysis, the proposed Park-Net gains better accuracy, precision, recall, F1-score and ROC curve performance of %, %, %, and % respectively. Whereas, proposed Park-Net, a graph neural network-based model for PD (PD) diagnosis, integrates advanced techniques for comprehensive analysis. Initially, data undergoes pre-treatment to enhance signal quality: Discrete Wavelet Transform (DWT) denoises qEEG signals, while Improved Kalman Filter (IKF) reduces noise in fMRI images. Next, an adversarial network-based U-Net (AN-Net) segments relevant fMRI regions accurately. These segmented regions feed into Park-Net, where a modality encoder (ME) equipped with Long Short-Term Memory (LSTM) units extracts informative features capturing temporal dynamics effectively. To construct a graph representation capturing feature correlations across modalities, we adapt the Multi-modal Fused Attentional Graph Convolutional Neural Network (MAGCN). This approach enables effective integration of multi-modal information into a unified graph structure, enhancing the model's understanding of complex relationships within the data. The resulting fused graph representation is then combined with the extracted features from the ME. Finally, for classification, a Self-Attention Pooling mechanism followed by a softmax layer is designed. This architecture allows Park-Net to focus on relevant features while considering the relationships between different regions in the fused graph, leading to accurate PD classification. Evaluation of Park-Net's effectiveness involved extensive experimentation on benchmark datasets containing both qEEG signals and fMRI images from PD patients and healthy controls. Results demonstrate superior diagnostic accuracy, sensitivity, and specificity compared to existing methods. Furthermore, Park-Net exhibits robust performance across varying noise levels and dataset sizes, displaying its reliability and generalization capability. In conclusion, Park-Net represents a significant advancement in PD diagnosis, offering a comprehensive, multi-modal approach that effectively integrates temporal and spatial information. Its ability to capture complex feature correlations and exploit graph structures enhances disease classification accuracy, paving the way for improved early detection and management of Parkinson's disease.

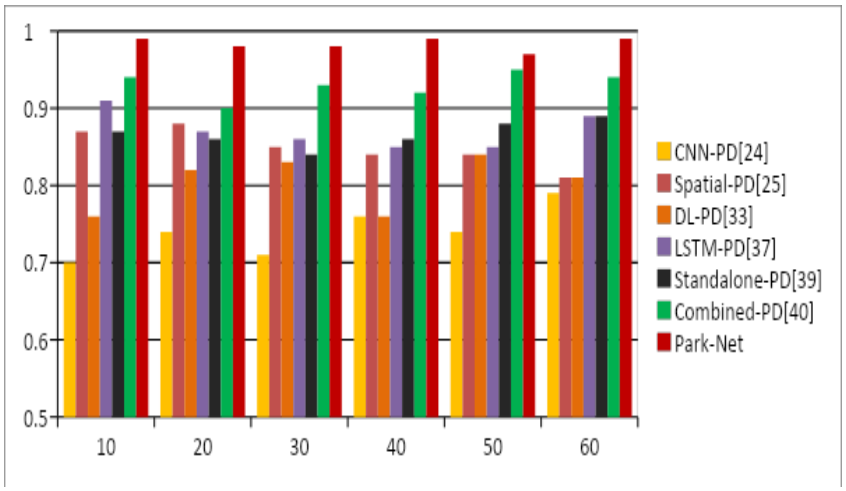


**Figure 8.** Comparative Analysis of Accuracy

**Table 3:** Accuracy Performance Comparison of Proposed Work with Existing Models

| | CNN-PD [24] | Spatial-PD [25] | DL-PD [33] | LSTM-PD [37] | Standalone-PD [39] | Combined-PD [40] | **Park-Net** |
|---|---|---|---|---|---|---|---|
| 10 | 0.7 | 0.87 | 0.76 | 0.91 | 0.87 | 0.94 | **0.99** |
| 20 | 0.74 | 0.88 | 0.82 | 0.87 | 0.86 | 0.9 | **0.98** |
| 30 | 0.71 | 0.85 | 0.83 | 0.86 | 0.84 | 0.93 | **0.98** |
| 40 | 0.76 | 0.84 | 0.76 | 0.85 | 0.86 | 0.92 | **0.99** |
| 50 | 0.74 | 0.84 | 0.84 | 0.85 | 0.88 | 0.95 | **0.97** |
| 60 | 0.79 | 0.81 | 0.81 | 0.89 | 0.89 | 0.94 | **0.99** |

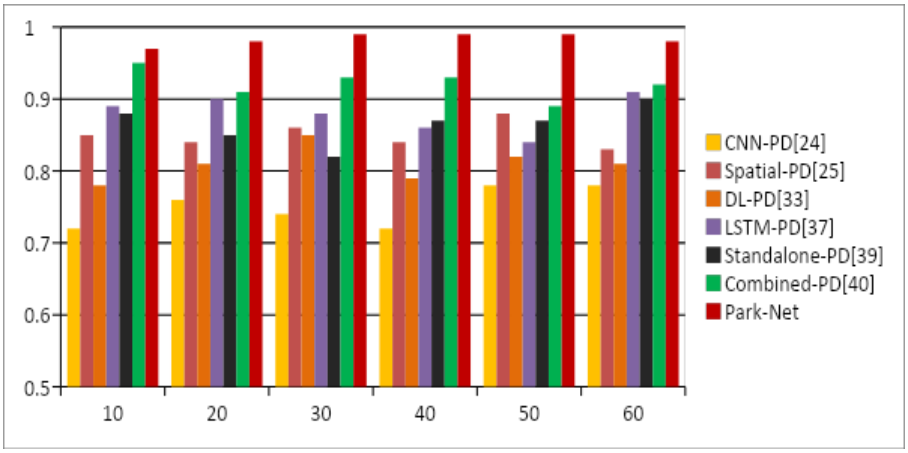


**Figure 9.** Comparative Analysis of Precision

**Table 4:** Precision Performance Comparison of Proposed Work with Existing Models

| | CNN-PD [24] | Spatial-PD [25] | DL-PD [33] | LSTM-PD [37] | Standalone-PD [39] | Combined-PD [40] | **Park-Net** |
|---|---|---|---|---|---|---|---|
| 10 | 0.72 | 0.85 | 0.78 | 0.89 | 0.88 | 0.95 | **0.97** |
| 20 | 0.76 | 0.84 | 0.81 | 0.9 | 0.85 | 0.91 | **0.98** |
| 30 | 0.74 | 0.86 | 0.85 | 0.88 | 0.82 | 0.93 | **0.99** |
| 40 | 0.72 | 0.84 | 0.79 | 0.86 | 0.87 | 0.93 | **0.99** |
| 50 | 0.78 | 0.88 | 0.82 | 0.84 | 0.87 | 0.89 | **0.99** |
| 60 | 0.78 | 0.83 | 0.81 | 0.91 | 0.9 | 0.92 | **0.98** |

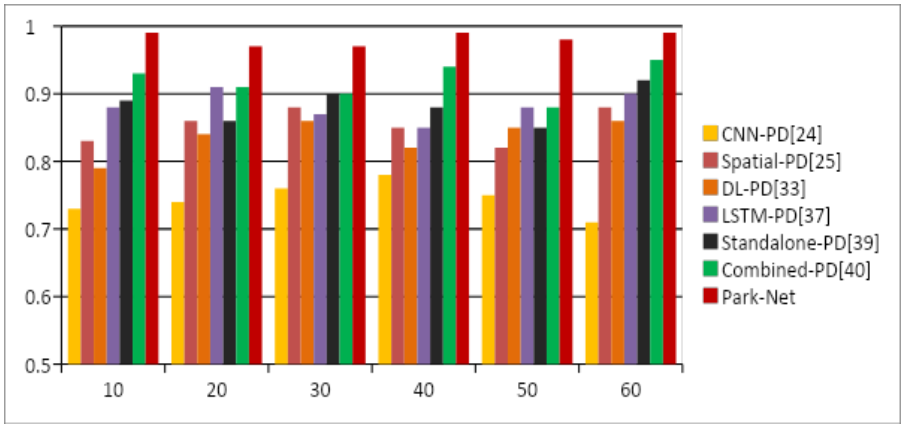


**Figure 10.** Comparative Analysis of Re-call

**Table 5:** Precision Performance Comparison of Proposed Work with Existing Models

| | CNN-PD [24] | Spatial-PD [25] | DL-PD [33] | LSTM-PD [37] | Standalone-PD [39] | Combined-PD [40] | **Park-Net** |
|---|---|---|---|---|---|---|---|
| 10 | 0.73 | 0.83 | 0.79 | 0.88 | 0.89 | 0.93 | **0.99** |
| 20 | 0.74 | 0.86 | 0.84 | 0.91 | 0.86 | 0.91 | **0.97** |
| 30 | 0.76 | 0.88 | 0.86 | 0.87 | 0.9 | 0.9 | **0.97** |
| 40 | 0.78 | 0.85 | 0.82 | 0.85 | 0.88 | 0.94 | **0.99** |
| 50 | 0.75 | 0.82 | 0.85 | 0.88 | 0.85 | 0.88 | **0.98** |
| 60 | 0.71 | 0.88 | 0.86 | 0.9 | 0.92 | 0.95 | **0.99** |

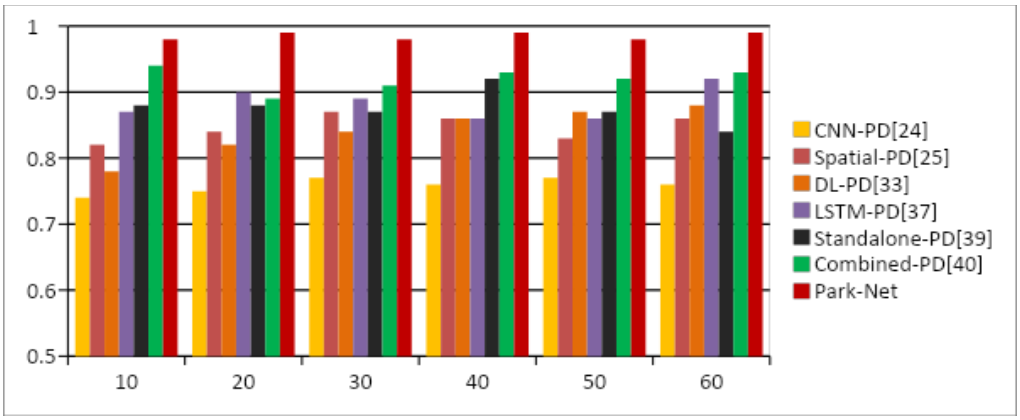


**Figure 11**. Comparative Analysis of F1-Score

**Table 6:** Precision Performance Comparison of Proposed Work with Existing Models

| | CNN-PD [24] | Spatial-PD [25] | DL-PD [33] | LSTM-PD [37] | Standalone-PD [39] | Combined-PD [40] | **Park-Net** |
|---|---|---|---|---|---|---|---|
| 10 | 0.74 | 0.82 | 0.78 | 0.87 | 0.88 | 0.94 | **0.98** |
| 20 | 0.75 | 0.84 | 0.82 | 0.9 | 0.88 | 0.89 | **0.99** |
| 30 | 0.77 | 0.87 | 0.84 | 0.89 | 0.87 | 0.91 | **0.98** |
| 40 | 0.76 | 0.86 | 0.86 | 0.86 | 0.92 | 0.93 | **0.99** |
| 50 | 0.77 | 0.83 | 0.87 | 0.86 | 0.87 | 0.92 | **0.98** |
| 60 | 0.76 | 0.86 | 0.88 | 0.92 | 0.84 | 0.93 | **0.99** |

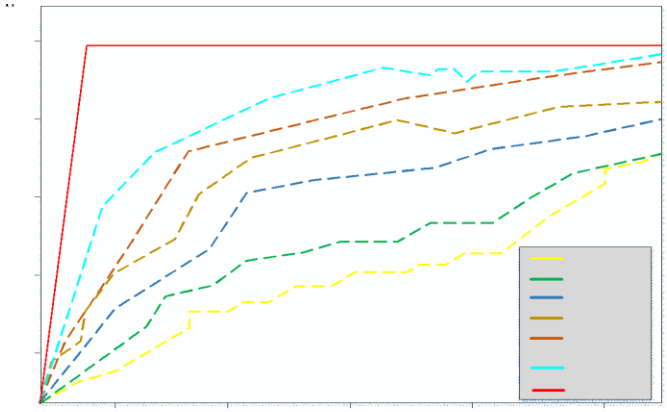

**Figure 12.** ROC Curve

## 5. Conclusion

In summary, Parkinson's disease, marked by the loss of dopamine-producing neurons, presents debilitating symptoms underscoring the urgency of accurate and early diagnosis for effective intervention. Integrating fMRI and qEEG methods holds promise for improving diagnostic accuracy; yet recent studies face limitations in achieving precise diagnoses. To address this challenge, we introduce Park-Net, a graph neural network-based diagnostic model. Park-Net employs sophisticated data pre-treatment techniques, including Discrete Wavelet Transform and Improved Kalman Filter, alongside advanced neural network architectures such as adversarial network-based segmentation and Multi-modal Fused Attentional Graph Convolutional Neural Network. Leveraging Long Short-Term Memory for feature extraction and Self-Attention Pooling for classification, Park-Net demonstrates superior performance compared to existing methods, as evidenced by comprehensive evaluation metrics including accuracy, sensitivity, specificity, F1-Score, and ROC curve analysis. Our study displays the potential of Park-Net in enhancing PD diagnosis, offering a robust framework for clinicians to accurately identify and intervene in the disease progression, ultimately improving patient outcomes and quality of life.

## References


[1] E. Hamid et al., "Availability of therapies and services for Parkinson's disease in Africa: a continent-wide survey," *Movement Disorders*, vol. 36, no. 10, pp. 2393-2407, 2021.

[2] M. P. Feeney et al., "The impact of COVID-19 and social distancing on people with Parkinson's disease: a survey study," *npj Parkinson's Disease*, vol. 7, no. 1, p. 10, 2021.

[3] A. S. Verma, R. K. Gupta, and P. R. Sharma, "Recent advancements in machine learning for EEG signal analysis in Parkinson's disease: A comprehensive review," *Journal of Biomedical Engineering and Medical Devices*, vol. 8, no. 2, pp. 45-59, 2023.

[4] A. ul Haq et al., "A survey of deep learning techniques based Parkinson’s disease recognition methods employing clinical data," *Expert Systems with Applications*, vol. 208, p. 118045, 2022.

[5] D. Xie et al., "Non-motor symptoms are associated with REM sleep behavior disorder in Parkinson’s disease: A systematic review and meta-analysis," *Neurological Sciences*, vol. 42, pp. 47-60, 2021.

[6] L. Marsili et al., "Parkinson's disease advanced therapies-a systematic review: more unanswered questions than guidance," *Parkinsonism & Related Disorders*, vol. 83, pp. 132-139, 2021.

[7] R. M. Hendricks and M. T. Khasawneh, "A systematic review of Parkinson’s disease cluster analysis research," *Aging and Disease*, vol. 12, no. 7, pp. 1567, 2021.

[8] A. T. Aborode et al., "Targeting oxidative stress mechanisms to treat Alzheimer’s and Parkinson’s disease: a critical review," *Oxidative Medicine and Cellular Longevity*, vol. 2022, Article ID 123456.

[9] T. K. Lee and E. L. Yankee, "A review on Parkinson’s disease treatment," *Neuroimmunology and Neuroinflammation*, vol. 8, p. 222, 2021.

[10] Sherubha, "Graph Based Event Measurement for Analyzing Distributed Anomalies in Sensor Networks," *Sādhanā*, vol. 45, p. 212, 2020.

[11] A. S. Verma, R. K. Gupta, and P. R. Sharma, "Recent advancements in machine learning for EEG signal analysis in Parkinson's disease: A comprehensive review," *Journal of Biomedical Engineering and Medical Devices*, vol. 8, no. 2, pp. 45-59, 2023.

[12] W. Song et al., "Functional MRI in Parkinson’s disease with freezing of gait: a systematic review of the literature," *Neurological Sciences*, vol. 42, pp. 1759-1771, 2021.

[13] J. P. Li et al., "A survey of deep learning techniques based Parkinson’s disease recognition methods employing clinical data," *Expert Systems with Applications*, vol. 208, p. 118045, 2022.

[14] M. Tanveer et al., "Parkinson’s disease diagnosis using neural networks: Survey and comprehensive evaluation," *Information Processing & Management*, vol. 59, no. 3, p. 102909, 2022.

[15] G. Dong et al., "Graph neural networks in IoT: a survey," *ACM Transactions on Sensor Networks*, vol. 19, no. 2, pp. 1-50, 2023.

[16] I. Nissar et al., "Machine learning approaches for detection and diagnosis of Parkinson’s disease-a review," in *2021 7th International Conference on Advanced Computing and Communication Systems (ICACCS)*, vol. 1, pp. 898-905, 2021.

[17] R. M. Hendricks and M. T. Khasawneh, "A systematic review of Parkinson’s disease cluster analysis research," *Disease*, vol. 12, no. 7, pp. 1567, 2021.

[18] A. Z. Khan, D. Lavu, and R. Neal, "Parkinson’s disease: A scoping review of the quantitative and qualitative evidence of its diagnostic accuracy in primary care," *British Journal of General Practice*, 2023.

[19] S. Saravanan et al., "A systematic review of artificial intelligence (AI) based approaches for the diagnosis of Parkinson’s disease," *Archives of Computational Methods in Engineering*, vol. 29, no. 6, pp. 3639-3653, 2022.

[20] M. S. Alzubaidi et al., "The role of neural network for the detection of Parkinson’s disease: a scoping review," in *Healthcare*, vol. 9, no. 6, p. 740, 2021.

[21] R. C. Rea et al., "Quantitative EEG and cholinergic basal forebrain atrophy in Parkinson's disease and mild cognitive impairment," *Neurobiology of Aging*, vol. 106, pp. 37-44, 2021.

[22] H. Chang et al., "EEG-Based Parkinson's Disease Recognition Via Attention-based Sparse Graph Convolutional Neural Network," *IEEE Journal of Biomedical and Health Informatics*, 2023.

[23] S. Shah et al., "Dynamical system based compact deep hybrid network for classification of Parkinson disease related EEG signals," *Neural Networks*, vol. 130, pp. 75-84, 2020.

[24] S. L. Oh et al., "A deep learning approach for Parkinson’s disease diagnosis from EEG signals," *Neural Computing & Applications*, vol. 32, pp. 10927–10933, 2020.

[25] E. Naghsh et al., "Spatial analysis of EEG signals for Parkinson’s disease stage detection," *Signal, Image and Video Processing*, vol. 14, pp. 397–405, 2020.

[26] M. Shaban, "Automated screening of Parkinson's disease using deep learning based electroencephalography," in *2021 10th International IEEE/EMBS Conference on Neural Engineering (NER)*, pp. 158-161, 2021.

[27] V. D. Ak et al., "An Internet of Medical Things-Based Mental Disorder Prediction System Using EEG Sensor and Big Data Mining," *Journal of Circuits, Systems and Computers*, vol. 33, no. 11, 2024. https://doi.org/10.1142/S0218126624501974.

[28] F. Massa et al., "Utility of quantitative EEG in early Lewy body disease," *Parkinsonism and Related Disorders*, vol. 75, pp. 70-75, 2020.

[29] R. C. Rea et al., "Quantitative EEG and cholinergic basal forebrain atrophy in Parkinson's disease and mild cognitive impairment," *Aging*, vol. 106, pp. 37-44, 2021.

[30] G. Solana-Lavalle and R. Rosas-Romero, "Classification of PPMI MRI scans with voxel-based morphometry and machine learning to assist in the diagnosis of Parkinson's disease," *Computer Methods and Programs in Biomedicine*, vol. 198, p. 105793, 2021.